Control of the Rate of Reverse Electron Transport in Submitochondrial Particles by the Free Energy†

Hagai Rottenberg*,‡ and Menachem Gutman

ABSTRACT: The effects of the substrates and products on the rate and direction of ATP-dependent reverse electron transport from succinate to nicotinamide adenine dinucleotide (NAD) in bovine heart submitochondrial particles (ETPH) were investigated. Except at very low and very high concentrations of the reactants (relative to their apparent K_ms), the rate of reverse electron transport depends linearly on log [ATP]/[ADP][phosphate] at constant redox potential and on log [reduced NAD][fumarate]/[NAD][succinate] at constant phosphate potential. The process can be converted from reverse to forward electron transport by poising the redox potential at appropriate values and lowering the phosphate potential. Similarly, poising the phosphate potential and increasing the redox potential convert reverse electron transport into forward electron transport. In the state with no net electron transport, the free-energy change associated with ATP hydrolysis is lower than the change associated with the redox reaction's free energy by 3 to 4 kcal/mol. This indicates that the stoichiometry ATP/2 e^- of the process is 1.3 or greater. These findings are discussed in relation to the chemiosmotic mechanism of coupling. It is suggested that the observed stoichiometry might be the result of an H^+/ATP ratio of 3 and an H^+/2 e^- ratio of 4 for the span succinate → NAD. The effect of uncouplers on adenosine triphosphatase (ATPase) and reverse electron transport and the effect of NADH on the rate of the ATPase reaction suggest that the intrinsic coupling in ETPH particles is quite tight, at least in the first site, despite their low P/O ratio and lack of respiratory control.

The observation of ATP[1]-dependent reduction of NAD by succinate in mitochondria (Chance and Hollunger, 1961) was the first indication that oxidative phosphorylation is reversible. The stoichiometric formation of acetoacetate by this reaction in mitochondria (Klingenberg and Hafen, 1963) and the stoichiometric reduction of NAD by succinate in submitochondrial particles demonstrated unequivocally that this process is indeed a reversal of oxidative phosphorylation (Löw et al., 1961; Löw and Vallin, 1963). The fact that antimycin A, in concentrations that completely inhibit electron transport through cytochrome *b*, caused only partial inhibition of reverse electron transport, and other less direct evidence (cf. papers and discussions in Chance, 1963), was interpreted as an indication that the reversal occurs only at the first phosphorylation site (Ernster and Lee, 1964). Thus, the process was considered as a stoichiometric coupling of the two reactions.

$$\text{succinate} + \text{NAD}^+ \rightleftharpoons \text{fumarate} + \text{NADH} + \text{H}^+ \quad (1)$$

$$\text{ATP} + \text{H}_2\text{O} \rightleftharpoons \text{ADP} + \text{P}_i \quad (2)$$

The overall reaction was written as:

$$\text{succinate} + \text{NAD}^+ + \text{ATP} + \text{H}_2\text{O} \rightleftharpoons \text{fumarate} + \text{NADH} + \text{H}^+ + \text{ADP} + \text{P}_i \quad (3)$$

In this study we investigate the effects of the substrates and products of reverse electron transport on the rate and direction of this process in submitochondrial particles from beef heart (ETPH). It is demonstrated that, within limitations, the kinetics of the coupled process are dictated by the free energy of the processes. The free-energy balance reveals that eq 3 is not a stoichiometric description of the process. A stoichiometric equation which is consistent with the free-energy balance is[2]:

$$\text{succinate} + \text{NAD}^+ + 4/3\text{ATP} \rightarrow \text{fumarate} + \text{NADH} + \text{H}^+ + 4/3\text{ADP} + 4/3\text{P}_i \quad (4)$$

The present conclusion that the transport of 2 electrons from succinate to NAD requires more than 1 ATP suggests a more complicated coupling scheme for oxidative phosphorylation than has been generally considered within the chemical or chemiosmotic mechanisms. These results could be accommodated by the chemiosmotic mechanism (Mitchell, 1968) either by revising the H^+/ATP and H^+/2 e^- ratios to 3 and 4, respectively, instead of 2 or by postulating that reverse electron transport at site I is assisted by site II.

Materials and Methods

Beef heart mitochondria were prepared on a large scale (Ringler et al., 1963) and frozen portions of this preparation were used to prepare submitochondrial particles of the ETPH type (Hansen and Smith, 1964). For each experiment a small portion of a frozen ETPH suspension was thawed and then incubated prior to the experiment with succinate and KCN at 30 °C to activate the succinic dehydrogenase (Gutman et al., 1971). Electron transport was measured by the formation or disappearance of NADH which was followed spectroscopically at 340 nm. Components of the reaction mixture were added to the suspension of submitochondrial particles prior to the addition of ATP which initiated the reaction. All reported rates are initial rates measured 3 to 5 s after the addition of ATP. The free energy of ATP hydrolysis (eq 2) was calculated from

† From the Biochemistry Department, The George S. Wise Center for Life Sciences, Tel-Aviv University, Ramat-Aviv, Tel-Aviv, Israel. *Received October 5, 1976.* Supported by a grant from the United States–Israel Binational Science Foundation.

‡ Present address: Bell Laboratories, Murray Hill, N.J.

[1] Abbreviations used are: ATP and ADP, adenosine tri- and diphosphates, respectively; NAD, nicotinamide adenine dinucleotide; NADH, reduced NAD; ATPase, adenosine triphosphatase; Tris, 2-amino-2-hydroxymethyl-1,3-propanediol.

[2] Equation 4 can be written in a dogmatic stoichiometric equation as 3 succinate + 3 NAD^+ + 4 ATP → 3 fumarate + 3 NADH + 3 H^+ + 4 ADP + 4 P_i.

the concentrations of added ADP, ATP, and phosphate, assuming a standard free-energy change ($\Delta G^{\circ\prime}_{ATP}$) of −7.20 kcal/mol (pH 7.4, 30 °C, I = 0.20, 5 mM Mg^{2+}) as extrapolated from the data of Rossing and Slater (1972).

$$\Delta G_{ATP} = \Delta G^{\circ\prime}_{ATP} + 1.38 \log \frac{[ADP][P_i]}{[ATP]} \quad (5)$$

The ATPase rate was measured in parallel to allow corrections for changes in concentrations during the course of the reaction. The ATPase activity was in the range of 200 to 600 nmol (mg of protein)$^{-1}$ min^{-1}. Since the concentration of ADP, ATP, and phosphate was above 200 μM in most experiments, the changes could be neglected. In a few experiments where 200 μM or less was used, corrections (of the order of 10 to 30 μM) were necessary. Since in most cases ADP, ATP, and P_i were in the mM concentration range, it was not necessary to consider the cross-contamination of these reagents which at most amounted to 1%. The myokinase activity of our particles is at least two orders of magnitude less than the ATPase activity and therefore could not significantly change the ATP/ADP ratios. In several experiments the particles were further washed, eliminating myokinase activity, while in other experiments ADP was added after ATP (thus changing the direction of the myokinase reaction). No significant differences were observed between these experiments and the standard experiments, indicating that myokinase does not significantly affect the ADP/ATP ratio under our conditions. Even if the myokinase reaction had been allowed to reach equilibrium, which was not the case, the maximal error in calculating ΔG_{ATP} would be 0.5 kcal/mol. The free energy of NAD reduction by succinate (eq 1), ΔG_{ox}, was calculated from the concentration of added succinate, fumarate, NAD, and the measured concentration of NADH, assuming a standard free-energy change ($\Delta G^{\circ\prime}_{ox}$) of +14.68 kcal/mol (pH 7.4, 30 °C, I = 0.20) extrapolated from the values compiled by Clark (1960).

$$\Delta G_{ox} = \Delta G^{\circ\prime}_{ox} + 1.38 \log \frac{[NADH][fumarate]}{[NAD][succinate]}$$

Succinate and fumarate were always in mM concentration and thus did not change significantly during the course of the measurements. Since NADH was followed continuously, any change in the NAD concentration could be accurately determined.

The ATPase activity was followed by measuring the release of protons according to the method of Nishimura et al. (1962) and corrected for either release or consumption of protons by the redox reaction.

Protein was determined by the biuret method (Layne, 1952) with bovine serum albumin as a standard.

All reagents were of analytical grade. ATP, Sigma grade, disodium; ADP (grade I), sodium salt; NAD; NADH; antimycin A; and oligomycin were from Sigma, and FCCP was a gift from Dr. P. G. Heytler of Du Pont Co. Wilmington, Del.

Results

Reverse electron transport was followed by the appearance of NADH in a suspension of ETPH particles which were preincubated with succinate, cyanide, and NAD. The reaction was initiated by the addition of the other components listed in the caption of Figure 1, the last being ATP. Figure 1 summarizes the effect of the ADP and P_i concentrations on the initial rate of reverse electron transport. Since the absolute maximal rate of different preparations varied (80–120 nmol min^{-1} (mg of protein)$^{-1}$), the results are normalized relative to the maximum rate. Both ADP and P_i inhibit reverse electron transport as previously observed (Löw and Vallin, 1963). However, over a wide concentration range the rate is linearly dependent on log [ATP]/[ADP][P_i]. This finding indicates that the rate is controlled to a large extent by the free-energy change of ATP hydrolysis, commonly referred to as "phosphate potential" (Klingenberg and Schollmeyer, 1961). Deviation from linearity was observed only at very high and very low phosphate potentials.

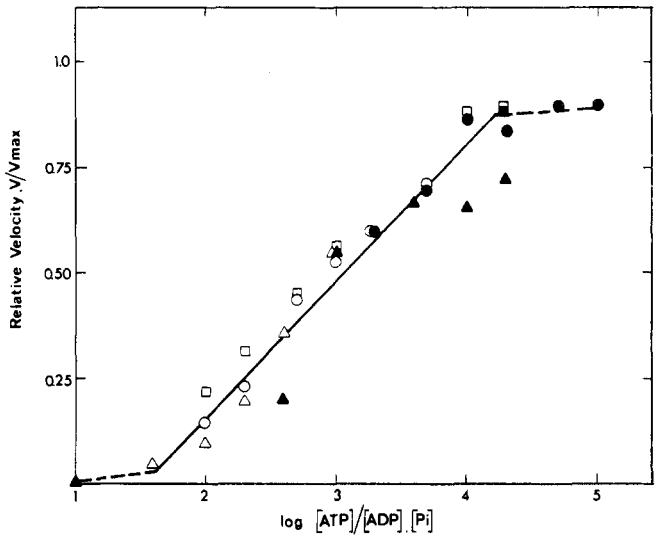

FIGURE 1: The effect of phosphate potential on the rate of NAD reduction by succinate. The incubation medium contained sucrose, 0.18 M; Tris-acetate, 50 mM (pH 7.4); $MgSO_4$, 5 mM; KCN, 1 mM; succinate, 5 mM; NAD, 1 mM; bovine serum albumin, 0.1%; ETPH particles, 0.6 mg/mL; and ADP and P_i, as indicated. The reaction mixture was preincubated at 30 °C for at least 5 min and was initiated by the addition of ATP (1 mM). The initial rate of NAD reduction was constant for at least 20 s. The data are expressed as relative rates, since the maximal activities of the different preparations were variable between 80–120 nmol min^{-1} mg^{-1}: (○) 0.1 mM ADP and P_i varied from 0.1 to 5.0 mM; (●) 0.1 mM ADP and P_i varied from 2.0 to 100 mM; (△) 0.5 mM ADP and P_i varied from 0.1 to 5.0 mM; (▲) 0.5 mM ADP and P_i varied from 2.0 to 100 mM; (□) P_i 1.0 mM and ADP varied from 0.05 to 50 mM.

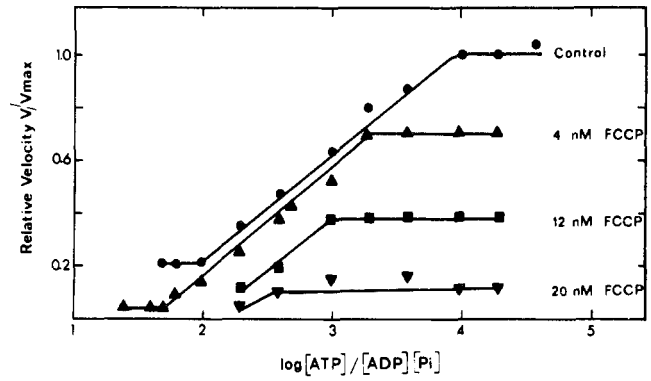

FIGURE 2: The effect of phosphate potential on the rate of NAD reduction by succinate at various degrees of uncoupling by FCCP. The reaction was measured under the same conditions as in Figure 1. In all experiments, ADP was 0.5 mM and P_i was varied between 50 μM and 100 mM. (●) No FCCP; (▲) 4 nM FCCP; (■) 12 nM FCCP; (▼) 20 nM FCCP.

Figure 2 shows similar experiments in the presence of increasing concentrations of the uncoupler FCCP. At any given phosphate potential, increasing concentrations of uncoupler inhibit reverse electron transport, which is of course the ex-

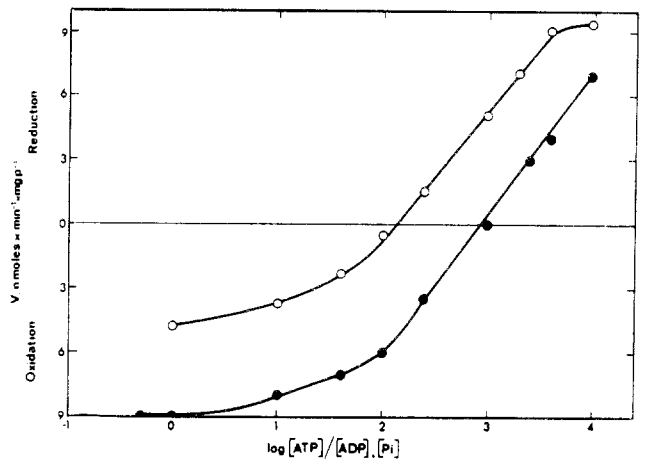

FIGURE 3: The effect of phosphate potential on the rate of NAD reduction and NADH oxidation at different redox potentials. The reaction was measured under the same conditions as in Figure 1, except for the concentration of NAD and succinate and the addition of fumarate and NADH. (○) Succinate, 30 mM; fumarate, 100 mM; NAD, 1 mM; NADH, 20 μM (ΔG_{ox} = 13.15 kcal/mol). (●) Succinate, 30 mM; fumarate, 100 mM; NAD, 0.1 mM; NADH, 20 μM; (ΔG_{ox} = 14.43 kcal/mol).

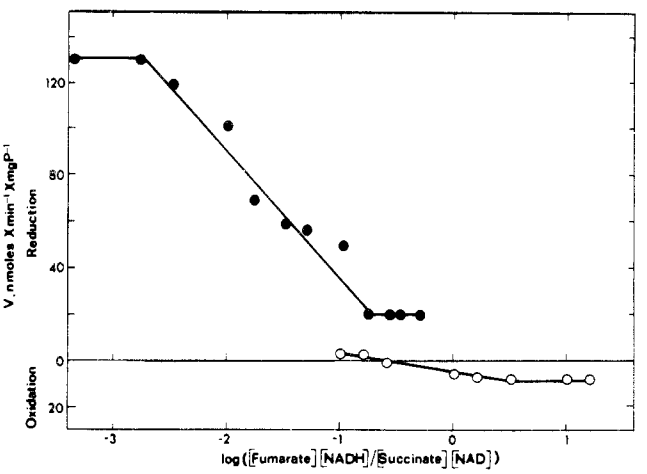

FIGURE 4: The effect of NADH on the rate of NAD reduction and NADH oxidation. Basic reaction medium as in Figure 1. (●) P_i, 0.2 mM; ADP, 0.5 mM; ATP, 1 mM (log [ATP]/[ADP][P_i] = 4.0); succinate, 20 mM; fumarate, 1 mM; NAD, 1 mM; and NADH, 30 μM to 7 mM. (○) P_i, 20 mM; ADP, 0.5 mM; ATP, 1 mM (log [ATP]/[ADP][P_i] = 2.0); succinate, 30 mM; fumarate, 10 mM; NAD, 0.1 mM; and NADH, 3 μM to 1 mM.

pected effect of an uncoupler. However, the proportionality between the uncoupler concentration and the inhibition of reverse electron transport is not the same at all values of phosphate potential. The inhibition is more pronounced at high phosphate potentials. As a result, the uncoupler shifts the leveling-off point of the rate to lower values of phosphate potential.

In the experiments of Figures 1 and 2, the redox potential was not clamped and was not precisely known, since neither fumarate nor NADH was added. Lowering the phosphate potential reduced reverse electron transport to very low values but no forward electron transport could be observed because of the absence of either fumarate or NADH. In Figure 3, the redox potential is clamped by the addition of NADH and fumarate. Lowering the phosphate potential decreases the rate of reverse electron transport which is converted to NADH–fumarate reductase (Sanadi and Fluharty, 1963). It should be emphasized that the NADH oxidation rate shown in Figure 3 is not an oxidase activity. It is a fumarate-dependent and antimycin + cyanide-insensitive reaction which can be accelerated by addition of uncoupler (now shown). The figure also shows that when the free energy of the redox system is clamped at a more positive value (○, ΔG_{ox} = +13.1 and ●, ΔG_{ox} = +14.4) the transition from forward to reverse electron transport requires a higher phosphate potential. Thus, it is clear that the redox potential affects both the direction and the rate of electron transport in this system. We therefore explored the effect of the redox potentials of donor or acceptor couples on the rate and direction of electron transport. Figure 4 shows the effect of NADH on the rate and direction of electron transport at two different phosphate potentials. At high phosphate potential (ΔG = −12.7 kcal/mol) and relatively low redox free energies (ΔG = +9.9 to +14.7; ●) increasing NADH concentration slows the rate of the reaction but does not change its direction. Saturation is reached before the balance of forces is tipped. However, when the phosphate potential is lowered (ΔG = −10 kcal/mol) and the redox free energy is higher (ΔG = +13.3 to +16.9 kcal/mol; ○) addition of NADH changes the direction from reverse to forward electron transport. Figure 5 shows a similar experiment at two different phosphate potentials in which the redox potentials of the donor couple were

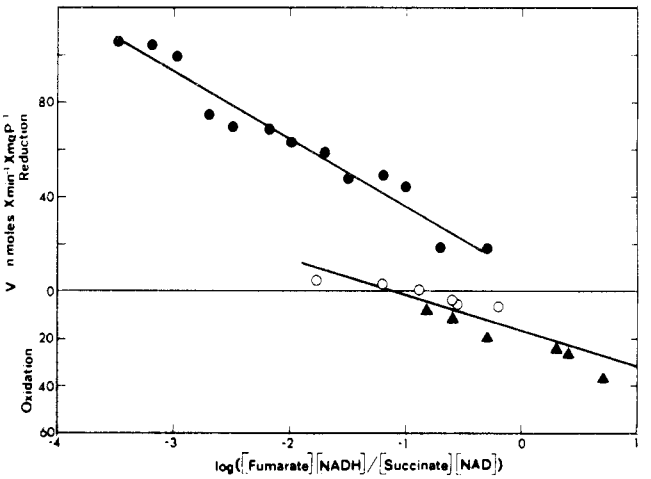

FIGURE 5: The effect of fumarate on the rate of NAD reduction and NADH oxidation. Basic reaction medium as in Figure 1. (●) P_i, 0.2 mM; ADP, 0.5 mM; ATP, 1 mM (log [ATP]/[ADP][P_i] = 4.0); succinate, 20 mM; NAD, 1 mM; NADH, 0.1 mM; and fumarate, 66 μM to 66 mM. (○) P_i, 20 mM; ADP, 0.5 mM; ATP, 1 mM (log [ATP]/[ADP][P_i] = 2.0); succinate, 20 mM; NAD, 1 mM; NADH, 0.1 mM; and fumarate, 33 μM to 10 mM. (△) Same as ○ except that succinate was 2 mM and fumarate varied from 3 mM to 100 mM.

varied by changing the fumarate concentration. Again electron transport changes directions only at low phosphate potential.

Figure 6 shows the effect of NAD concentration on the rate and direction of electron transport at low phosphate potential. Increasing the concentration of NAD shifts the reaction from forward to reverse electron transport. The results of the experiments of Figures 3–6 suggest that the rate of reverse electron transport is mainly controlled by the redox and phosphate potentials. When the concentration of the various reactants are of the same order of magnitude as the K_ms, only thermodynamic control is observed. This is illustrated in Figure 7 where the redox potential was varied over a range of 4 kcal/mol. Yet, when the rate is plotted against log ([NADH][fumarate]/[NAD][succinate]) all the points fit a straight line, showing that the rate of electron transport in both direc-

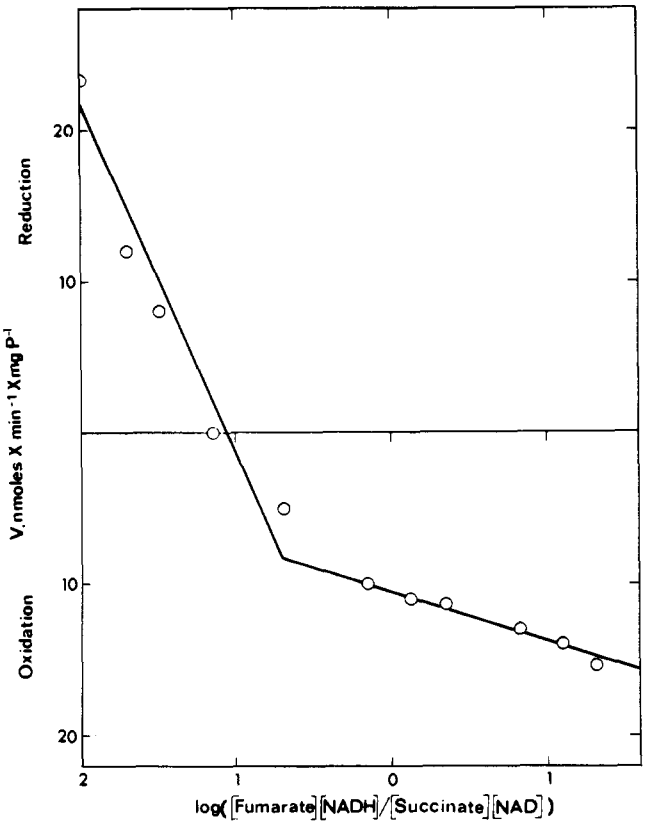

FIGURE 6: The effect of NAD on the rate of NAD reduction and NADH oxidation. Conditions are as in Figure 1 except that P_i was 0.2 mM, ADP was 0.5 mM, and ATP was 1 mM (log [ATP]/[ADP][P_i] = 2.0) succinate was 30 mM, fumarate was 100 mM, NADH was 20 μM, and NAD was varied from 3 μM to 5 mM.

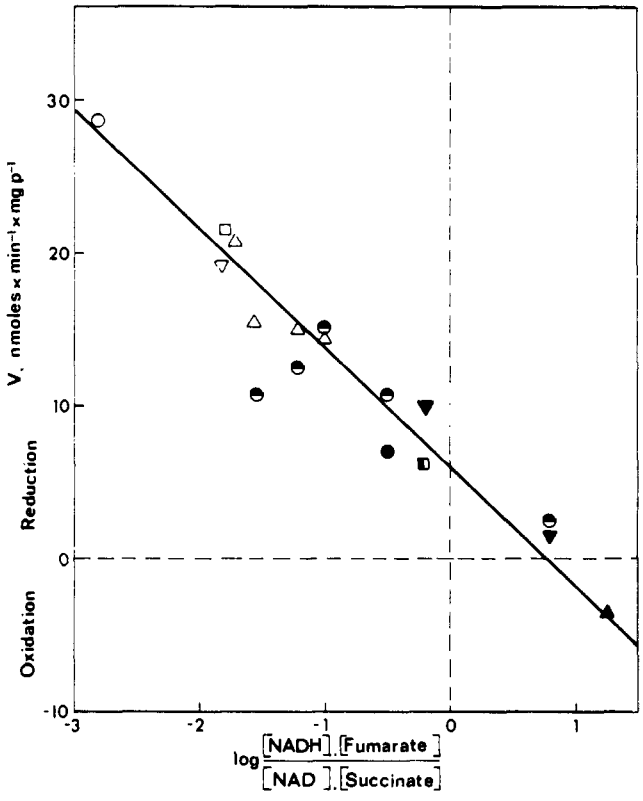

FIGURE 7: The dependence of the rate of reverse electron transport on the redox gap between donor and acceptor couples. The rate of the reaction was measured as described before using 1 mM ATP to initiate the reaction; the concentrations of the component varied within the ranges: succinate, 1-20 mM; fumarate, 1-20 mM; NAD, 0.03-1 mM; NADH, 0.03-0.2 mM. The concentrations of fumarate and succinate are given in mM, as follows: (▲) 20, 5; (▼) 10, 5; (●) 10, 1; (◓) 10, 10; (▽) 5, 20; (◧) 1, 5; (□) 25, 20; (△) 1, 10. The NADH/NAD ratio was varied to obtain the redox potentials indicated on the abscissa. In the absence of fumarate and NADH the rate was 40.5 mol min^{-1} (mg of protein)$^{-1}$.

tions is a linear function of the redox potential. However, the different slopes and deviations from linearity at extreme conditions indicate that kinetic parameters also determine the rate of electron transport.

The intersection of the abscissa by the curves shown in Figures 3 to 7 represents states in which there is no net electron transport. Each such point is characterized by a particular set of values of phosphate and redox potentials. The ATPase reaction at these particular states still proceeds, though at a lower rate (see Figure 9). These states are equivalent, in the reverse electron transport domain, to state 4 of oxidative phosphorylation. In this state the free energy at ATP hydrolysis maintains the maximal redox potential difference between the donor couple and the acceptor couple. An increase of the redox potential gap results in oxidation of NADH, while any decrease results in reverse electron transport. Similarly, in state 4 of oxidative phosphorylation the phosphate potential is at a maximum and any increase in phosphate potential results in ATP hydrolysis and decrease in ATP synthesis.[3]

Figure 8 shows a plot of values of ΔG_{ox} against ΔG_{ATP} at the state of maximal ΔG_{ox} of reverse electron transport. These values are taken from the experiments of Figures 3 through 7 and from other similar experiments over a wide range of values of ΔG_{ox} and ΔG_{ATP}. In all cases, ΔG_{ox} is larger than ΔG_{ATP} by 3 to 4 kcal/mol. The average of the ratio $\Delta G_{ox}/\Delta G_{ATP}$ is 1.35 ± 0.09 SD (n = 19). It is clear therefore that more than 1 mol of ATP must be hydrolyzed per mol of NAD reduced.

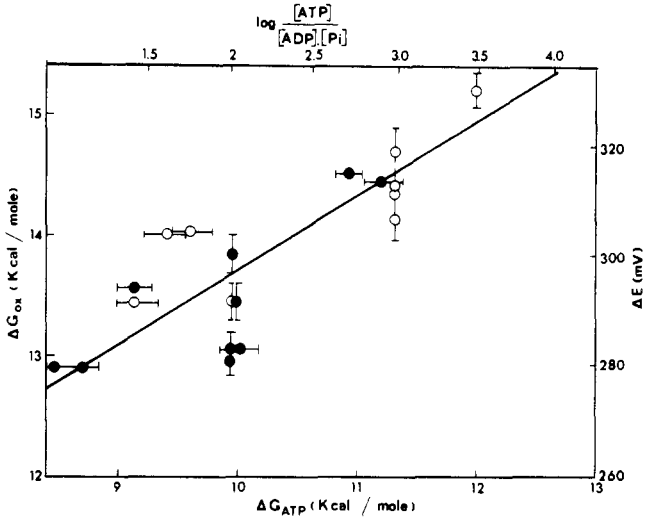

FIGURE 8: Correlation between redox potential and phosphate potential at maximal ΔG_{ox}. The figure summarizes results of 19 experiments as in Figures 3, 4, 5, and 6. In experiments where the phosphate potential was held constant and the redox potential was varied, the experimental error of the maximal ΔG_{ox} is drawn parallel to the ordinate. In experiments where the phosphate potential varied and the redox potential was constant, the experimental error of the phosphate potential is drawn parallel to the abscissa. The phosphate potential was varied by changing the concentrations of ATP (0.5-1 mM), ADP (0.1-2 mM), and P_i (1-20 mM). The ratio NADH/NAD was varied between the range of 0.03 and 1.8, and fumarate/succinate between 0.1 and 10.

[3] These states are referred to as "static head" in the terminology of nonequilibrium thermodynamics (see Discussion). For clarity, we would refer to this state here as the state of maximal ΔG_{ox}.

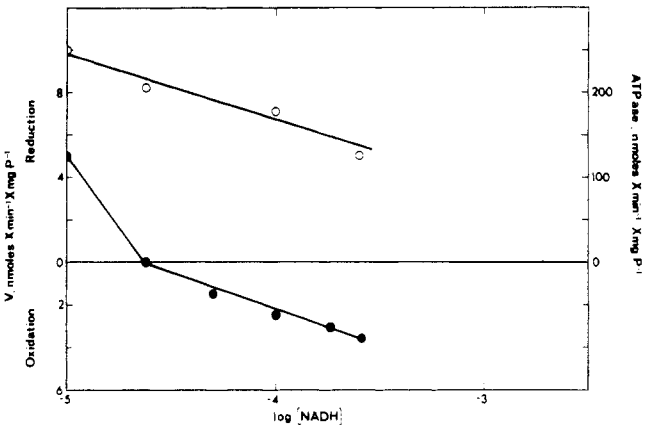

FIGURE 9: The effect of NAD concentration on rate of NAD reduction and of ATPase. Basic medium as in Figure 1, except that Tris-acetate was replaced by potassium acetate. P_i, 20 mM; ADP, 0.5 mM; ATP, 1 mM (log [ATP]/[ADP][P_i] = 2.0); succinate, 12 mM; fumarate, 12 mM; NAD, 0.5 mM; and NADH, 10 μM to 0.2 mM. ATPase was followed by the release of protons as described under Methods. (●) Electron transport; (○) ATPase.

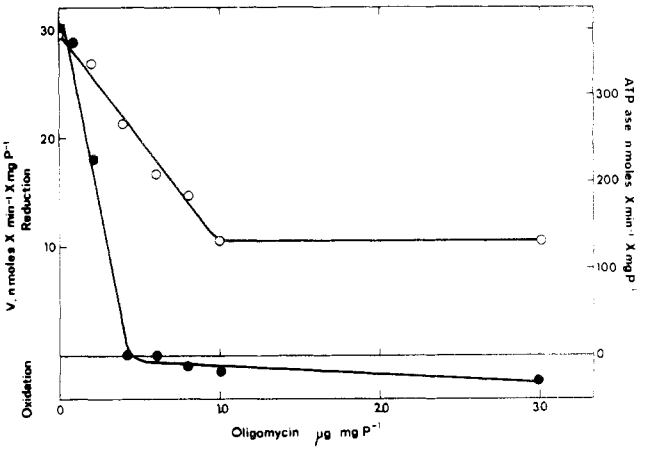

FIGURE 10: The effect of oligomycin on NAD reduction, NADH oxidation, and ATPase. Conditions are as in Figure 9, except for the NADH concentration which was 50 μM.

The minimal stoichiometry compatible with our findings is 4/3 mol of ATP per mol of NAD, as expressed in eq 4.

Figure 9 shows the effect of added NADH (as in Figure 4) both on the rate of the ATPase and the rate of electron transport. It must be emphasized that, since these experiments are carried in a state very close to the maximum value of ΔG_{ox}, the rate ratio is extremely high and can give no indication of the stoichiometry. Indeed, when ΔG_{ox} is maximal, reverse electron transport vanishes and the ratio becomes infinite. Nevertheless, it is observed that not only the rate of electron transport is controlled by the redox potential but also the rate of the ATPase is inhibited as the redox potential becomes negative. This behavior is indicative of a rather tight coupling between the two processes (similar to the control of electron transport by phosphate potential in oxidative phosphorylation). However, the fact that ATPase proceeds at a rather high rate when electron transport vanishes and even at the region of forward electron transport indicates that the coupling, though tight, is not complete. Even at conditions more favorable to reverse electron transport, i.e., high phosphate potential and less positive redox potential, the rate of the ATPase is at least three to four times higher than the rate of reverse electron transport (not shown). This is probably due to a rather large component of ATPase activity which is oligomycin-insensitive and presumably totally uncoupled. The existence of this activity is demonstrated in Figure 10 which shows the effect of oligomycin on electron transport and ATPase. It is observed that increasing oligomycin concentration similarly inhibits ATPase and reverse electron transport until the spontaneous fumarate reductase takes place. The fraction of the ATPase which is oligomycin insensitive contributes to the high activity of ATPase observed during reverse electron transport. The ATPase activity at the state of maximal ΔG_{ox} was inhibited to about 50% by oligomycin. Figure 11 shows the effect of FCCP on reverse electron transport and ATPase. As expected, uncoupling inhibits reverse electron transport and at saturation reverses the direction of electron transport. In parallel, we observe a 170% increase of ATPase activity, indicating that a large portion of the ATPase is tightly coupled.

Discussion

The relationship between redox free energy, ATPase free energy, and the direction and rate of electron transport in submitochondrial particles is described in this study. Of particular interest is the state of maximal ΔG_{ox} in reverse electron transport which is described and analyzed in detail. An unexpected finding is that in the state of maximal ΔG_{ox} of reverse electron transport the positive free-energy value of the electron transport reaction is 3 to 4 kcal/mol higher than the ATPase free energy. Even if the system were completely coupled (which it is not, see below), one expects that on initiating reverse electron transport in this state $\Delta G_{ox}/\Delta G_{ATP} \leq 1$ if the stoichiometry were unity (eq 3). Yet in all cases $\Delta G_{ox}/\Delta G_{ATP} > 1$. Since in submitochondrial particles ATP hydrolysis, succinate oxidation, and NAD reduction all occur at the external membrane surface, the internal concentration of the reactants are not relevant. Since the external concentration of all reactants was known quite accurately, the observed differences in free energy were real and are not due to experimental or computational error. Our findings indicate that the stoichiometry must be greater than 1; the lowest stoichiometric factor compatible with our result is 1.35 (Figure 8). Here we suggest two alternative explanations for our findings: (a) that the second site is involved, (b) that the ratio at each site, in submitochondrial particles, is 1.33.

The Involvement of the Second Site. It is known that the antimycin concentration which completely blocks respiration causes only partial inhibition (~20%) of the NADH-fumarate reductase and the energy-linked NAD reduction by succinate (Sanadi and Fluharty, 1963) (Homes, 1963a,b, Hass, 1964). This indicates that for such reactions electron transport in the b-c region is not necessary, but it does not exclude the possibility that energy-linked electron transport in the b-Q region assists in NAD reduction by succinate. If such a mechanism operates, it will affect the stoichiometry of eq 3.

The reverse electron transport in site I can be equated with the ATP-dependent, uncoupler-sensitive, oxidation of the iron-sulfur center 2 of NADH dehydrogenase. This reaction is observed in the presence of piericidin which prevents equilibration of center 2 with the quinone (Gutman et al., 1972). If piericidin is absent, then ATP causes a reduction of center 2. This reduction might correspond to the 100-mV shift of the redox potential observed when redox mediators are present (Ohnishi, 1976) but much smaller, only 30 mV, when substrates (succinate and fumarate) are the redox buffer (Gutman et al., 1975). This shift is too small to be attributed to a transducing carrier, but suffice to act as accessory mechanism to narrow to redox potential gap between centers 2 and 1. Whether this occurs by cycling of electrons from the domain

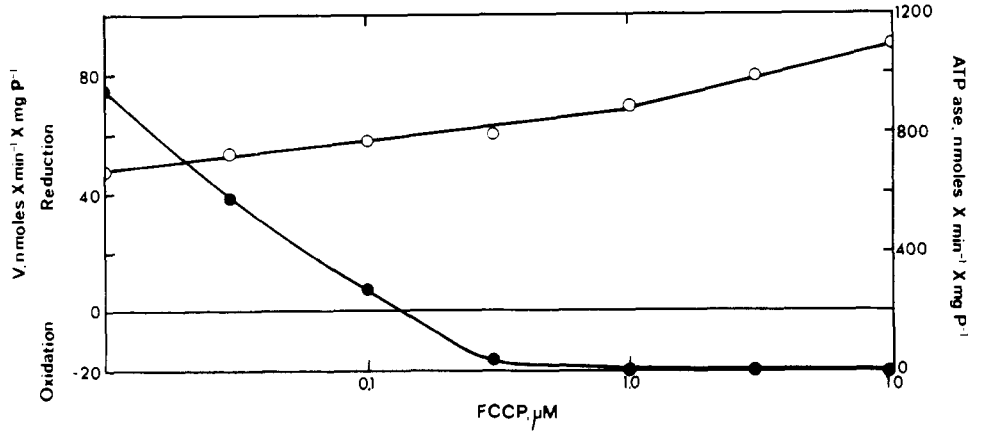

FIGURE 11: The effect of FCCP on NAD reduction, NADH oxidation, and ATPase. Conditions are as in Figure 9, except for: succinate, 5 mM; fumarate, 5 mM; NAD, 0.3 mM; NADH, 0.1 mM; ATP, 1 mM.

of CoQ associated with succinate dehydrogenase (Gutman and Silman, 1972) to cytochrome *b* and back to NADH dehydrogenase domains of CoQ or whether it represents the different potentials of the $OH_2 \rightleftarrows QH$ and $OH \rightleftarrows Q$ reactions in center *i* of the Q cycle (Mitchell, 1976) is still to be investigated. Presently, to evaluate this possibility we are studying the effect of electron transport inhibition on the reverse reaction.

The ATP/2 e⁻ Ratio at Each Site Is Greater Than One. We find this alternative particularly attractive within the context of the chemiosmotic model. The original suggestion for the chemiosmotic mechanism is that at each site 2 protons are transported per 2 e^- while 2 H^+ are transported back for each ATP synthesized, giving an overall stoichiometry at each site of 1 ATP/2 e^- (Mitchell, 1968). Recently, however, it was suggested by various investigators that these stoichiometries must be revised upward. From comparison of $\Delta\tilde{\mu}_H$ and phosphate potential it was suggested that at least 3 H^+/ATP are transported by the ATPase (Rottenberg, 1975, 1977). Similarly, reinvestigation of the H^+/O ratio has indicated that the H^+/2 e^- ratio at each site might be as high as 4 (Brand et al., 1976). If indeed these are the stoichiometries 3 H^+/ATP and 4 H^+/2 e^- per site then the overall ATP/2 e^- stoichiometry per site should be 1.33, which agrees very well with our experimental findings. It should be pointed out that based on these values the stoichiometry of 1.33 ATP per site is expected only in submitochondrial particles which are inverted. In mitochondria an additional proton is required for the transport of ADP and P_i into the mitochondria and the transport of ATP out, as discussed elsewhere (Klingenberg, 1975). Recent investigation of the relationship between $\Delta\tilde{\mu}_H$ and reverse electron transport in ETPH particles show that at the state of maximal ΔG_{ox}, $\Delta\tilde{\mu}_H$ is equivalent to 3.4 kcal/mol under conditions where ΔG_{ATP} is 10 kcal/mol and ΔG_{ox} is 13.6 kcal/mol (Rottenberg, unpublished). Hence, $\Delta G_{ATP}/\Delta\tilde{\mu}_H = 2.9$ and $\Delta G_{ox}/\Delta\tilde{\mu}_H = 4.0$ which agrees very well with the stoichiometries of 3 H^+/ATP and 4 H^+/2 e^- as suggested here.

The Kinetics of a Complex-Coupled System—a Nonequilibrium Description. At least three very large membrane-bound enzyme complexes are involved in the process of reverse electron transport: succinic dehydrogenase, NADH dehydrogenase, and ATPase. Each of these contains numerous distinct proteins and other active components. The reactions within each of these complexes are still mostly not known at the molecular level. Moreover, the interactions between the electron carriers and the ATPase constitute the elusive mechanism of oxidative phosphorylation. It is therefore clear that any attempt to describe the kinetics of the overall process in terms of sequential molecular interactions is premature.

The kinetic behavior of a complex-coupled system such as oxidative phosphorylation or reverse electron transport can be described in two alternative ways. The kinetic approach is to describe the system in terms of conventional enzyme kinetics where the effect of the substrates and products is due to the mass-action law. Thus, the transition in oxidative phosphorylation from the high respiration rate in state 3 to state 4 is assumed to reflect either the limiting amounts of the substrates (ADP or P_i) or product inhibition by ATP (Chance and Williams, 1956). The limitation of this approach is the lack of a true kinetic model. Thus, it defines a set of apparent constants where all of them are interlocked and reflects the concentrations of more than one component. This severely limits the usefulness of this approach.

We have previously shown that within a certain domain of reactant concentrations (dictated by the real kinetic constants) the rate of an enzymatic reaction is a linear function of the reaction free energy (Rottenberg, 1973). Within this domain the kinetic description is equivalent to the alternative thermodynamic description. This latter description is particularly useful for complex-coupled systems of energy transfer (Rottenberg, 1973, 1977). In this study we have shown that the rate of reverse electron transport in beef heart submitochondrial particles is a function of the free energy of the process over a wide range of concentrations for each reactant. Moreover, the rate was a linear function of the free energy over an extended range of values. In Figures 1 through 6 the deviations from linearity are observed whenever the concentrations of the reactants are considerably below or above their apparent K_ms. However, when the free energy is varied over a wide range, but within the same order of magnitude as the apparent K_m for each component, the relationship between the free energy and the rate is strictly linear as in Figure 7. Within this domain the linear equations of nonequilibrium thermodynamics can be used to describe the coupled system as discussed elsewhere (Rottenberg, 1977). In terms of the mechanism of the coupling, these findings indicate that under most conditions a coupling intermediate is controlled by both electron transport and phosphorylation and is, in turn, controlling the rate of both reactions. If, for instance, the coupling is mediated by the proton electrochemical gradient ($\Delta\tilde{\mu}_H$) as suggested by Mitchell (1968) then our results suggest that $\Delta\tilde{\mu}_H$ would depend both on the redox potential and the phosphate potential, while the rates of electron transport and ATP hydrolysis would be controlled by $\Delta\tilde{\mu}_H$.

In describing the energetics of a coupled process it is gen-

erally assumed that the process is completely coupled (cf. Wilson and Ercinska, 1972). This is a necessary assumption for a quantitative treatment within the framework of equilibrium thermodynamics. Any deviation from the expected behavior, i.e., variable stoichiometry or lack of true equilibrium, is explained by unrelated or "uncoupled" activity, and often corrected by a simple substraction. We have pointed out (Rottenberg et al., 1967, 1970; Rottenberg, 1977) that this approach may lead to a serious erroneous conclusion regarding the stoichiometry of the reactions. Thus, in our view, state 4 of oxidative phosphorylation and the state of maximal ΔG_{ox} of reverse electron transport are not equilibrium states, as assumed for a completely coupled process, but rather a steady state of minimal entropy production. The fact is that when the driven process is halted, the driving process still proceeds and it is the free energy and the rate of this latter reaction as well as the degree of coupling that determines the magnitude of the free energy of the driven force. That is, in the partially coupled system of reverse electron transport, it is the ongoing ATPase which maintaines the maximal redox potential. An analysis of energy conversion which is based on nonequilibrium thermodynamics (Kedem and Caplan, 1965) defines as "Static head" the state in which the free energy of the driven process is maximum (positive) and its rate has vanished. In this state entropy production is minimal. The state of maximal ΔG_{ox} in reverse electron transport is shown here to be a "Static head", since in this state ATPase (eq 2) holds a maximal positive free energy of NAD reduction by succinate (eq 1) while its rate has vanished. Another illustration of such a state is "State 4" of oxidative phosphorylation. Truly, there is also an uncoupled, oligomycin-insensitive ATPase activity at "Static head", but a considerable activity at this state is coupled as is necessary for the maintenance of the redox potential. Because reverse electron transport is only partially coupled and because of the rather high oligomycin-insensitive activity, the process stoichiometry cannot be estimated from the rate ratio of this reaction. The procedure used previously (cf. Klingenberg and Hafen, 1963; Löw et al., 1963; Ernster and Lee, 1964) which subtracts the rate of ATPase in the absence of reverse electron transport from the rate of the ATPase during electron transport cannot be justified in view of the discussion above. A similar calculation for oxidative phosphorylation in ETPH particles gives P/O ratios which are often higher than the expected maximum. In our ETPH preparation the P/O with succinate is at best 0.7, while the respiratory control ratio is 1.2. If we apply the correction method of subtracting the "basal" respiration rate, we get a "corrected" ratio, 0.7/0.2 = 3.5, almost twice as high as the expected ratio.

It is generally agreed that ETPH particles are less coupled than mitochondria. This concensus is based on the fact that, normally, P/O ratios are very low in ETPH, respiratory control is hardly observed, and the ATPase activity is very high. Our results show a surprisingly tight control of the rate of the ATPase reaction both by the redox potential and by FCCP. Since we are studying reverse electron transport through the first site, we might be tempted to conclude that the first site is more coupled than the other sites. Another explanation is that the high rate of the "intrinsic uncoupled" oligomycin-insensitive ATPase affects the apparent coupling in oxidative phosphorylation experiments where the ATPase activity is not saturated but has a lower effect on the apparent coupling in reverse electron transport under conditions where the ATPase reaction is saturated. Whatever the reason for the low P/O and respiratory control in ETPH, the fact that the reverse electron transport proceeds at very low phosphate potentials and the fact of tight control of the ATPase reaction indicate a surprisingly high degree of coupling for reverse electron transport.

Acknowledgment

We thank R. Copel for her technical assistance.

References

Brand, M. D., Reynafarje, B., and Lehninger, A. L. (1976), *Proc. Natl. Acad. Sci. U.S.A. 73,* 437.

Chance, B., Ed. (1963), Energy Linked Function of Mitochondria, New York, N.Y., Academic Press.

Chance, B., and Hollunger, G. (1961), *J. Biol. Chem. 236,* 1534.

Chance, B., and Williams, G. R. (1956), *Adv. Enzymol. Relat. Subj. Biochem. 17,* 92.

Clark, W. M. (1960), Oxidation-Reduction Potentials of Organic Systems, Baltimore, Md., Williams and Wilkins.

Ernster, L., and Lee, C. P. (1964), *Annu. Rev. Biochem. 33,* 729.

Flatmark, F., and Pedersen, J. I. (1973), *Biochim. Biophys. Acta 325,* 16.

Gutman, M., Beinert, M., and Singer, T. P. (1975), in Electron Transfer Chains and Oxidative Phosphorylation, Quagliariello et al., Ed., Amsterdam, North-Holland Publishing Co., p 55.

Gutman, M., Kearney, E. B., and Singer, T. P. (1971), *Biochemistry 10,* 4763.

Gutman, M., and Silman, N. (1972), *FEBS Lett. 26,* 207.

Gutman, M., Singer, T. P., and Beinert, H. (1972), *Biochemistry 11,* 556.

Hansen, M., and Smith, L. A. (1964), *Biochim. Biophys. Acta 81,* 214.

Hass, D. W. (1964), *Biochim. Biophys. Acta 92,* 433.

Hommes, F. A. (1963a), *Biochim. Biophys. Acta 77,* 173.

Hommes, F. A. (1963b), *Biochim. Biophys. Acta 77,* 183.

Kedem, O., and Caplan, S. R. (1965), *Trans. Faraday Soc. 61,* 1897.

Klingenberg, M. (1975), *Ciba Found. Symp. 31,* 105.

Klingenberg, M., and Hafen, H. V. (1963), *Biochem. Z. 337,* 120.

Klingenberg, M., and Schollmeyer, P. (1961), *Biochem. Z. 335,* 231.

Layne, E. (1952), *Methods Enzymol. 3,* 450-451.

Löw, H., Krueger, H., and Ziegler, D. M. (1961), *Biochem. Biophys. Res. Commun. 5,* 231.

Löw, H., and Vallin, I. (1963), *Biochim. Biophys. Acta 69,* 361.

Löw, H., Vallin, I., and Alm, B. (1963), in Energy Linked Function of Mitochondria, Chance, B., Ed., New York, N.Y., Academic Press.

Mitchell, P. (1968), Chemiosmotic Coupling and Energy Transduction, Bodmin, U.K., Glynn Research Ltd.

Mitchell, P. (1976), *J. Theor. Biol.* (in press).

Nishimura, M., Ito, T., and Chance, B. (1962), *Biochim. Biophys. Acta 59,* 177.

Ohnishi, T. (1976), *Eur. J. Biochem. 64,* 103.

Ringler, R. L., Minakami, S., and Singer, T. P. (1963), *J. Biol. Chem. 238,* 801.

Rosing, J., and Slater, E. C. (1972), *Biochim. Biophys. Acta 267,* 275.

Rottenberg, H. (1973), *Biophys. J. 13,* 503.

Rottenberg, H. (1975), *J. Bioenerg. 7,* 61.

Rottenberg, H. (1977), in Progress in Surface and Membrane Science, Danielli, J. F., Cadenhead, A., Rosenberg, M. D.,

Ed., New York, N.Y., Academic Press, in press.
Rottenberg, H., Caplan, S. R., and Essig, A. (1967), *Nature (London) 216,* 610.
Rottenberg, H., Caplan, S. R., and Essig, A. (1970), in Membranes and Ion Transport, Vol. 1, Bittar, E. E., Ed., New York, N.Y., Wiley, p 165.
Sanadi, D. R., and Fluharty, A. L. (1963), *Biochemistry 2,* 523.
Wilson, D. F., and Ercinska, M. (1972), *Fed. Eur. Biochem. Soc. Meet., Proc. 28,* 119.

Light-Activated Amino Acid Transport Systems in *Halobacterium halobium* Envelope Vesicles: Role of Chemical and Electrical Gradients†

Russell E. MacDonald,* Richard V. Greene, and Janos K. Lanyi‡

ABSTRACT: The accumulation of 20 commonly occurring L-amino acids by cell envelope vesicles of *Halobacterium halobium,* in response to light-induced membrane potential and an artificially created sodium gradient, has been studied. Nineteen of these amino acids are actively accumulated under either or both of these conditions. Glutamate is unique in that its uptake is driven only by a chemical gradient for sodium. Amino acid concentrations at half-maximal uptake rates (K_m) and maximal transport rates (V_{max}) have been determined for the uptake of all 19 amino acids. The transport systems have been partially characterized with respect to groups of amino acids transported by common carriers, cation effects, and relative response to the electrical and chemical components of the sodium gradient, the driving forces for uptake. The data presented clearly show that the carrier systems, which are responsible for uptake of individual amino acids, are as variable in their properties as those found in other organisms; i.e., some are highly specific for individual amino acids, some transport several amino acids competitively, some are activated by a chemical gradient of sodium only, and some function also in the complete absence of such a gradient. For all amino acids, Na^+ and K^+ are both required for maximal rate of uptake. The carriers for L-leucine and L-histidine are symmetrical in that these amino acids are transported in both directions across the vesicle membrane. It is suggested that coupling of substrate transport to metabolic energy via transient ionic gradients may be a general phenomenon in procaryotes.

Vesicles prepared from cell envelope membranes of *Halobacterium halobium* by sonication possess features characteristic of the membranes of whole cells; i.e., they have the same orientation as whole cell membranes, they contain purple membrane patches which function in light to pump protons across the membrane, they couple light energy to the formation of ion and electrical gradients, and they accumulate amino acids against large concentration gradients (MacDonald and Lanyi, 1975; Lanyi et al., 1976a,b; Kanner and Racker, 1975). In contrast to whole cells, light-induced ATP formation cannot be demonstrated in these vesicles using the most sensitive techniques available (Lanyi et al., 1976b). A number of workers (Berger and Heppel, 1974; Harold, 1976) have reported that amino acid transport in other bacteria, e.g., *Escherichia coli,* appears to be energized in at least two ways: one in which transport is the result of a protonmotive force or energized membrane state, and the other which directly involves the hydrolysis of ATP. Neither leucine nor glutamate transport in *H. halobium* vesicles is affected by added ATP, or arsenate inside or outside of the vesicles, and it therefore seems unlikely that ATP synthesis (or hydrolysis) is required for transport in vesicles. Whether ATP synthesis (or hydrolysis) is involved in transport in whole cells is not clear.

We have previously reported on the energetics of membrane transport for leucine (MacDonald and Lanyi, 1975) and glutamate (Lanyi et al., 1976a,b) in these vesicles and have shown that the driving force for leucine transport can be separated conceptally into two components, an electrical potential ($\Delta\Psi$)[1] which is generated by the light-activated proton pump (Oesterhelt, 1975), and a chemical sodium gradient (ΔNa^+)[1] which is generated via a Na^+/H^+ antiport system (Lanyi and MacDonald, 1976). Glutamate, in contrast, is transported only in response to a chemical sodium gradient.

The mechanism and structure of bacteriorhodopsin, the proton pump, has been the subject of extensive investigation (Bogomolni and Stoeckenius, 1974; Henderson and Unwin, 1975; Oesterhelt and Stoeckenius, 1973; Racker and Stoeckenius, 1973) but only a limited number of other reports (Kanner and Racker, 1975; Hubbard et al., 1976) have ap-

† From Section of Biochemistry, Molecular and Cell Biology, Division of Biological Sciences, College of Agriculture and Life Sciences, Cornell University, Ithaca, New York 14853. *Received November 17, 1976.* This work was supported in part by funds provided by the Cornell University Agricultural Experiment Station, in part by a research grant from the National Aeronautics and Space Administration, NSG-7235, in part by a NASA-Ames Life Sciences Faculty Research Participation award to R.E.M., and in part by NIH Grant GM 23225-01.

‡ Biological Adaptation Branch, Ames Research Center, National Aeronautics and Space Administration, Moffett Field, California 94035.

[1] Symbols and abbreviations used: $\Delta\Psi$, electrical potential across membrane; ΔpH, ΔNa^+, and ΔK^+, chemical gradients across membrane of H^+ (expressed at pH), Na^+, and K^+, respectively; Hepes, *N*-2-hydroxyethylpiperazine-*N'*-2-ethanesulfonic acid; Tris-HCl, tris(hydroxymethyl)aminomethane hydrochloride; ESR, electron spin resonance.